



Erosion Mapping of Coated Composites: Simulating Conditions for Tidal Turbines Blades

Emadelddin Hassan¹ · Margaret M. Stack¹

Received: 9 August 2024 / Revised: 30 December 2024 / Accepted: 2 January 2025
© Crown 2025

Abstract

The tribological mechanisms of potential composite materials that could be used in tidal turbines considered the effects of various erosion parameters on the degradation modes, both with and without particles, in still and seawater conditions. The aim of this study was to investigate the potential of a specialised epoxy erosion-resistant coating for glass fibre-reinforced plastic (GFRP) in resisting the impact of slurry erosion. Slurry erosion is a process by which solid particles suspended in a fluid medium impinge on a surface, causing material loss due to repeated impacts. The coating efficacy was evaluated through a series of tests, including three different speeds and six different impinging angles and the results were used to generate tidal turbine maps. The study provided insights into the durability and of the epoxy and potential use of the coating in tidal turbine blade industries where resistance to erosion is crucial for long-term performance and safety.

Keywords Erosion mapping · Polymeric coatings · Tidal energy · Glass fibre-reinforced polymer (GFRP) · Impact velocity

1 Introduction

Surface coatings have significant potential to reduce wear and erosion [1]. In studies of erosion in marine renewable energy systems, such as tidal turbine blades, there have been some recent studies on blade durability in laboratory-simulated erosion conditions using a range of experimental protocols [1–3]. In these experimental conditions, important parameters such as impact angle, velocity (relating to thrust loading), and particle concentration at the surface interface can be evaluated.

Such research is important as tidal energy is increasingly viewed as an important energy resource in the renewable energy spectrum [4]. However, the high-water densities encountered in blade impact test the current materials and surface engineering approaches. Understanding the mechanics of failure will provide understandings into materials selection in such conditions.

Very few studies in recent years have concentrated on erosion resistance in the presence of surface coatings. Such surface engineering approaches are key to extending longevity of the turbine blades. Tailoring the coatings to the environment is the route to preventing failure at interfaces in the material.

In this study, a coating was applied to a standard GRP composite and tested in simulated tidal erosion conditions over a spectrum of impact angles and velocities. The results have indicated a very significant difference in erosion mechanism with impact angle. Microscopy and erosion maps were used to identify modes of erosion and mechanisms of degradation.

2 Materials and Methodologies

2.1 Materials

The materials used in this study include FR4-G10 GRP, which serves as the base for the erosion-resistant coating being evaluated. These materials were selected for their unique properties and suitability for the intended purpose of the study. Technical specifications for each of these materials are provided in Table 1, which includes information on their mechanical, thermal, and water absorption properties.

✉ Emadelddin Hassan
Emadelddin.hassan@strath.ac.uk

Margaret M. Stack
Margaret.stack@strath.ac.uk

¹ Department of Mechanical & Aerospace Engineering,
University of Strathclyde, Glasgow G1 1XQ, UK

Table 1 Technical specifications of FR4-G10 GRP

Technical data	Units	Test method	Values
Colour	NA	NA	Light Green
Specific Gravity	g/cm ³	ISO 1183	1.95
Water Absorption	mg	ISO 62	5.5
Flexural Strength	MPa	ISO 178	500
Tensile Strength	MPa	ISO 527	450

Table 2 Coating specifications

Properties	Unit
Colour	Green
Hardness	ASTM typical value 87
Heat resistance	40 °C
Tensile strength	ASTM D412 15.2 MPa
Tear strength	ASTM D624 380 pli
Density	1.1 g/cm ³
Water absorption	nil

To ensure consistent and accurate testing, the materials were prepared by cutting sheets of plate arranged in a specific size of 36 mm by 25 mm and 3 mm thickness. The sheets were cut to fit into the Jet rig specimen holder which is used to direct the slurry at the coated samples. The uniformity and precision of the sample size and arrangement ensure that the results of the tests are reliable and repeatable.

The FR4-G10 GRP materials as a base for the coating is based on their durability, strength, and erosion resistance, which are essential properties for withstanding the impact of slurry erosion.

Overall, the use of these materials in the study ensures that the results obtained are applicable to real-world scenarios and can provide insights into the efficacy of the epoxy erosion-resistant coating for protecting materials from slurry erosion in various industries.

2.2 Coating Composition

Belzona 2141 is a high-performance, erosion resistance polymeric coating manufactured by Belzona International Ltd, which was selected for testing in this study due to its mechanical properties and high erosion resistance as described in Table 2.

To apply the Belzona 2141 coating to the FR4-G10 GRP samples, the surface of the samples was first prepared using 80-grit sandpaper, which helps to ensure good adhesion between the coating and the composite material. The Belzona 2911 activator was then mixed with the Belzona 2141 coating to achieve the required polymeric coating. This mixture was carefully prepared according to the manufacturer's

instructions to ensure the correct ratio of components and consistency of the coating [5].

Once the samples were prepared and the coating mixture was ready, the coating was applied as a one-coat system by brush [1, 5] to achieve the desired thickness. The coating application process was carried out under the supervision of Belzona representatives to ensure that it was performed correctly and according to the manufacturer's guidelines [5].

After application, the coated samples were left to dry for 24 h in ambient temperature conditions to allow the coating to cure and reach its full mechanical properties. The coating thickness was measured to ensure that the average thickness of 0.8 mm was achieved for all samples.

The application process for the Belzona 2141 coating involved careful preparation and application to ensure that the coating was evenly applied and had the required thickness and mechanical properties. The use of this high-performance coating in the study provides valuable insights into its effectiveness in protecting composite materials from slurry erosion in various industrial applications.

2.3 Impingement Rig Test Set-Up

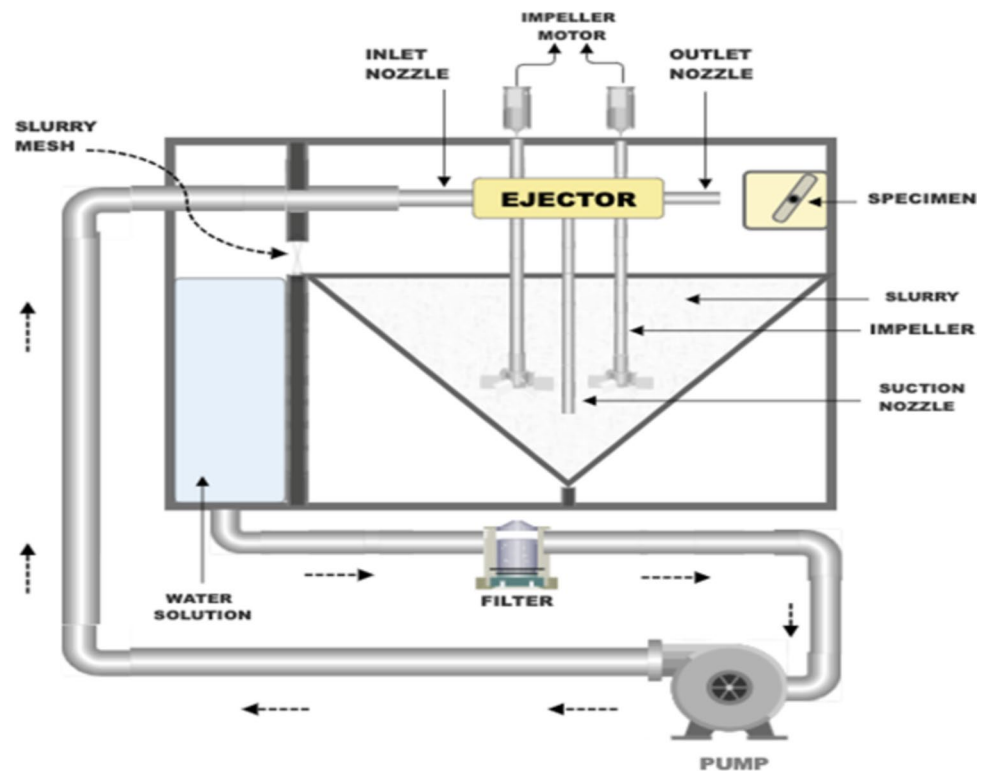
The experimental setup features a custom-designed slurry jet rig as shown in Fig. 1, constructed following the guidelines of Hutchings [6]. It consists of a polypropylene conical trapper for efficient sand recirculation, a T-shaped nozzle for slurry generation, and propellers driven by electric motors to ensure uniform mixing and circulation of the slurry. The rig's configuration allows for precise adjustment of parameters, such as slurry flow velocity and impingement angle, whilst operational guidelines dictate a maximum testing duration of 30 min to prevent pump overheating.

2.4 Test Conditions

The erosive characteristics were assessed through the examination of mass reduction utilising an analytical balance with a precision of ± 0.01 mg, coupled with a surface analysis conducted using a Scanning Electron Microscope (SEM). The experimental parameters, including impact angles, velocities, test duration, sand concentration, salinity, and test temperature, are summarised in Table 3.

Prior to each calibration, the rig was thoroughly prepared by filling it with clean water and running the pump for 5 min. This ensured that the system was flushed and free from residual sand particles or solution from previous experiments, thereby eliminating potential sources of contamination or measurement inaccuracies.

The velocities used in the tests were precisely regulated by varying the inlet nozzle diameters, as detailed in Table 4. To ensure the accuracy and reliability of these velocity measurements, the experimental rig was subjected to a systematic

Fig. 1 Impingement Rig Test Set-Up**Table 3** Test parameters

Parameter	Values
Impact Angles	15°, 30°, 45°, 60°, 75°, 90°
Impact Velocities	6.25 m/s, 8.42 m/s, 10.16 m/s
Test Duration	30 min per sample
Sand Concentration	3%
Salinity	3.5%
Sand Particle Size	300–600 μm
Test Temperature	Room temperature

Table 4 Nozzles vs velocities

Nozzle Inlet Dia (mm)	Test velocity (m/s)
2	6.25
2.5	8.42
3	10.16

calibration process. This involved first measuring the initial volume of water in the rig. The pump was then activated, and the elapsed time for a predefined volume of water to pass through the system was recorded. The final volume of water collected in a separate container was measured, and the net volume of water that passed through the rig was calculated by subtracting the initial volume from the final volume.

The statistical analysis employed in this study ensured the reliability of the results through the use of MATLAB to develop erosion maps for various conditions. Customised codes were created to process the experimental data and visualise material loss across different impact angles and velocities. Mean values from repeated experiments were calculated to minimise variability, whilst standard deviation quantified measurement dispersion, ensuring consistency and repeatability. The erosion maps integrated multiple datasets, allowing for a robust evaluation of trends and relationships, reducing the influence of experimental noise and enhancing the reliability of the study's conclusions.

The flow velocity (v) was determined using the following equation:

$$v = \frac{Q}{A}, \quad (1)$$

where ' v ' is the velocity, ' Q ' is the flow rate, and ' A ' is a cross-sectional area of the flow path. The volumetric flow rate (Q) was calculated by dividing the measured water volume by the elapsed time, whilst the cross-sectional area (A) was determined based on the nozzle dimensions.

To improve measurement precision and reduce uncertainty, the calibration procedure was repeated three times under identical conditions. The mean velocity values were calculated to provide a reliable representation of

the system's performance. This approach ensured that the velocity measurements were both accurate and repeatable, forming a robust basis for evaluating erosion mechanisms during subsequent experiments.

The rigorous calibration process, coupled with the preparatory flushing step, ensured that the experimental setup delivered consistent and reliable data, thereby supporting the validity of the findings presented in this study.

3 Results and Discussion

3.1 Results

The erosion of the coating material was significantly influenced by the impact angle and water flow velocity, according to Fig. 2 it was noted that the coating experienced higher mass loss at impact angles of 60° and 90°, regardless of the velocity. This suggests that these angles are more critical for the durability of the coating and should be considered in the design and operation of turbines.

Additionally, the results showed that lower velocities of 6.25 m/s caused less damage to the coating material than the higher velocities of 8.42 m/s and 10.16 m/s. This suggests that an element in the erosion of the coating material is velocity. Moreover, it was noticed that at an impact angle of 45°, the coating experienced mass loss at velocities of 8.42 m/s and 10.16 m/s.

The results of this experiment could have significant implications for the design and operation of tidal turbines. Erosion of the coating material can lead to reduced efficiency and a shorter lifespan of the turbines [2].

3.2 Effect of Velocities and Impact Angle on Coating

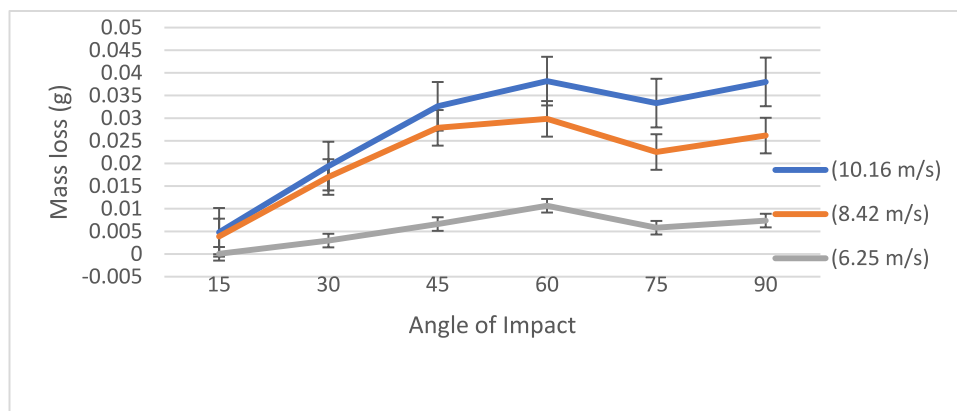
The performance of the tidal turbine relies on the rotor blade, which is a critical component for extracting kinetic energy from the tide stream [7]. The blade is similar in concept to a wind turbine blade, but its design and reliability assessment

cannot be based on those of the wind turbine due to differences in seawater density and other factors [1]. However, the efficiency and reliability of the blades are key indicators for a tidal current turbine [8]. The tribological issue, such as leading-edge erosion due to sand particles' impact, cavitation erosion, and the combined effects of seawater and solid particles, can compromise the performance and reliability of the rotor blade [1, 3]. Researchers have investigated the erosion of the rotor blade caused by the impact of erodent under marine simulated conditions, i.e. saltwater plus sand particles, but ignored erosion due to cavitation [1, 9, 10] also notes that the use of thermoplastic composite blades in a large-scale tidal power turbine is a potential game-changer for the marine energy industry, improving performance and sustainability, whilst also making the manufacturing process faster and more energy efficient.

The impact angle and velocity can significantly affect the erosion of polymeric coatings applied to tidal turbine blades [4, 11]. The erosion losses were evaluated at various impingement angles (15°–90°) and with the change of impact velocity 6.25 m/s, 8.42 m/s, and 10.16 m/s, which reflects typical velocities experienced at the leading edge of the blade [4]. The polymeric coating acts as a barrier between the substrate and NaCl solution, slowing the ingress of moisture in composite materials [1]. The impact frequency can affect the ability of a coating to absorb and distribute the energy from an impact [12], which is typically taken into account in current blade coating systems.

The results indicate that the impact angle and velocity have a significant effect on the erosion of the samples [13]. At all velocities, the coating experienced higher mass loss at 60° and 90° impact angles. This can be attributed to the fact that at these angles, the impact energy is concentrated on a smaller area, leading to a higher erosion rate. At 6.25 m/s, the coating experienced a lower mass loss compared to 8.42 m/s and 10.16 m/s, indicating that lower velocity leads to a lower erosion rate. However, at higher velocities of 8.42 m/s and 10.16 m/s, the coating experienced higher mass loss, indicating that higher velocity leads to a higher

Fig. 2 Mass Difference of Coated samples at 6.25 m/s, 8.42 m/s, and 10.16 m/s



erosion rate. At 45° impact angle, the coating experienced mass loss at velocities 8.42 m/s and 10.16 m/s, indicating that at this angle, higher velocities lead to a higher erosion rate. These results highlight the importance of considering impact angle and velocity when studying erosion and can be useful in designing coatings or materials that are more resistant to erosion [14].

Moreover, the coating material's ability to absorb and distribute the energy from an impact can also vary [12]. This further emphasises the importance of selecting the appropriate coating material and application process that can withstand the impact and erosion caused by the water flow. Overall, it is crucial to consider various factors, such as impact angle, velocity, and coating material properties [15, 16], when designing and operating tidal turbines to ensure the longevity and efficiency of the system.

3.3 SEM Analysis

A focused beam of high-energy electrons is used in a scanning electron microscope (SEM) to image the topography and learn about the material composition of conductive specimens. [17]. The SEM consists of an electron gun, a system of magnetic lenses, a scan control, and a detector, which work together to focus the electron beam on the sample and generate high-resolution images of its surface [17].

Salt deposition and particle embedding on coated GFRP surfaces, as observed in Fig. 3, have a significant impact on the long-term performance and structural integrity of the material. Salt enters the coating through diffusion into surface voids and pores, where it crystallises over time, causing localised stress concentrations and microcracking. This weakens the fibre–matrix interface, leading to delamination and exposure of reinforcement fibres, which accelerates degradation. Similarly, solid particles, such as sand, become embedded within the material surface during testing, contributing to mass gain [11]. This embedded material increases surface roughness, promotes localised stresses, and exacerbates mechanical wear.

These combined effects alter the surface properties of the coating, reducing its hydrodynamic efficiency and making it more susceptible to wear. To address these issues, coatings with lower porosity and improved resistance to salt and particle retention are necessary. Regular cleaning to remove salt deposits and embedded particles, coupled with real-time monitoring to detect surface changes, is essential for maintaining coating performance. Studies have shown that salt deposition and particle embedding act synergistically to accelerate damage under marine conditions, highlighting the importance of optimising coatings and maintenance strategies to ensure the durability of tidal turbine applications [18–20].

Figure 4 shows the results of an erosion test on a coating surface, specifically at a 75° angle and a velocity of 8.42 m/s. Figure 4 indicates that this impact caused significant damage to the coating, as evidenced by the presence of voids, cavities, and loose debris scattered around the eroded surface.

The specific impact angle of 75° and a velocity of 8.42 m/s are significant because they provide information about the strength and durability of the coating. The voids and cavities in Fig. 4 indicate that the impact caused the coating material to fracture and break apart. This type of damage can weaken the structural integrity of the coating and may compromise its ability to provide protection to the underlying material or surface [21]. The loose debris from sand and broken fibres scattered around the impact site suggests that the force of the impact was strong enough to dislodge and scatter coating material beyond the immediate vicinity.

Figure 5 confirms the presence of loose debris and coating erosion due to deformation and cutting action at a higher impact velocity of 10.16 m/s and an impact angle of 90°. The figure also confirms the ductile cutting in the coating at these test conditions [22].

The presence of loose debris indicates that the impact caused some material to be dislodged or broken apart, similar to what was observed in Fig. 5. The confirmation of loose debris and coating erosion at higher impact conditions suggests that the coating may not be able to withstand high-speed impacts at these conditions. The presence of ductile cutting in the coating further confirms that the coating is a ductile material, as was observed in Fig. 6 at lower impact conditions [23].

The combination of loose debris and cutting observed in Fig. 5 provides evidence of the extent of damage caused by the impact at these higher impact conditions. The deformation and cutting action caused significant damage to the coating, resulting in the removal of material and the formation of loose debris.

The confirmation of ductile cutting at higher impact conditions is significant because it suggests that the coating may undergo significant plastic deformation before fracturing [24].

This information is important for understanding the behaviour of the coating under high-speed impact conditions and for determining the potential applications of the coating in environments with high-speed impacts.

Figure 6 shows that at an impact angle of 75° and a velocity of 10.16 m/s, the coated surface suffered from pit propagation due to the impact of the erodent. The figure also shows the presence of loose debris and ductile cutting.

The observation of pit propagation is significant because it suggests that the impact caused the coating to undergo significant material removal in the form of pits. The presence

Fig. 3 SEM micrograph and EDX-coated sample at 15° Impact angle and 6.25-m/s velocity

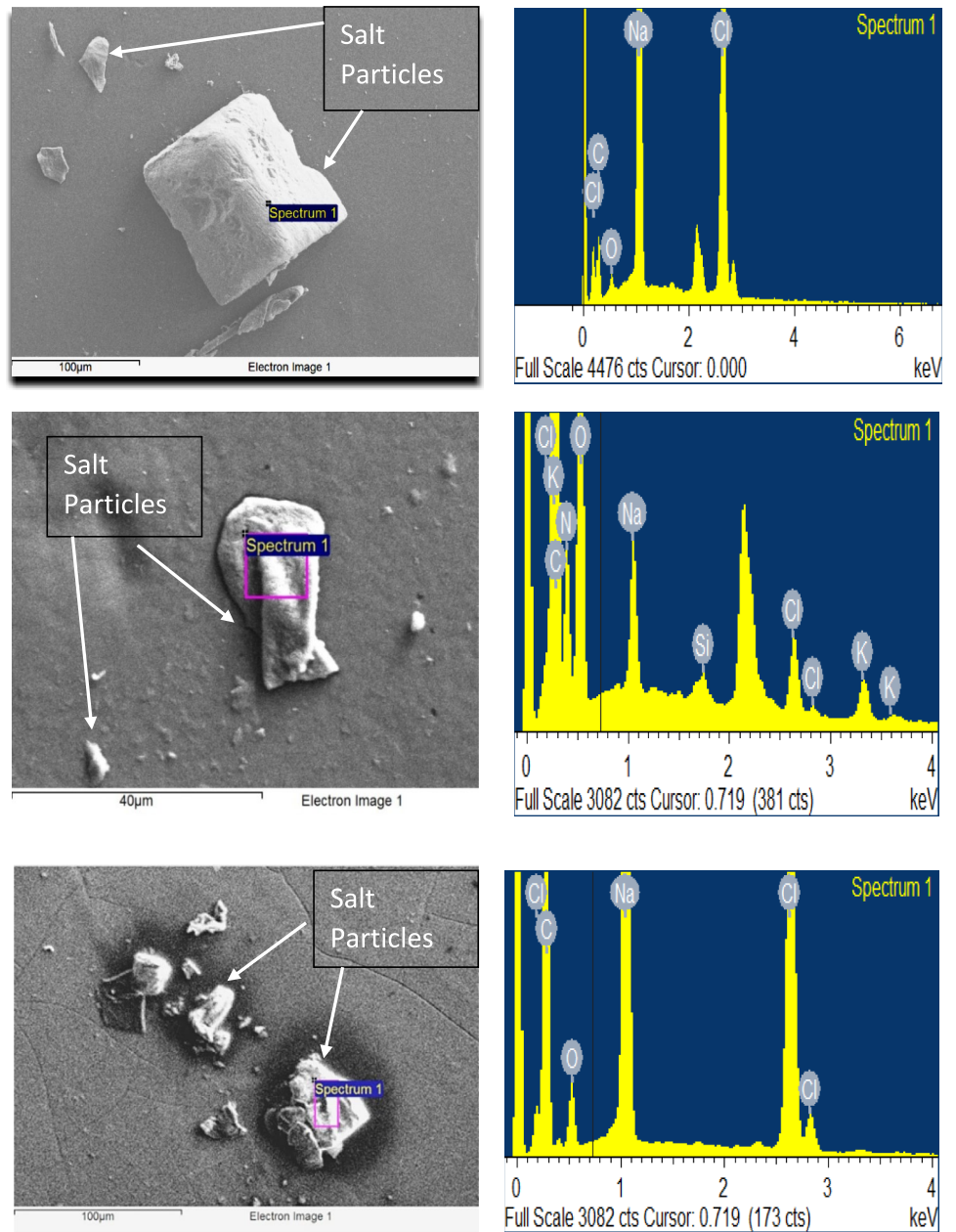


Fig. 4 Coated sample at 75° Impact angle and 8.42-m/s velocity



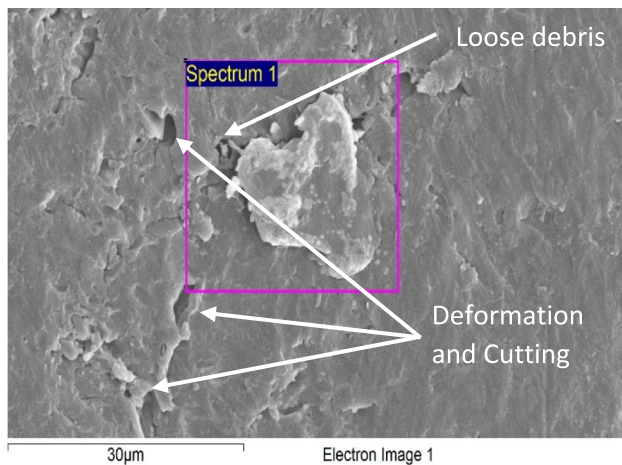


Fig. 5 Coated sample at 90 Impact angle and 10.16-m/s velocity

of loose debris and ductile cutting further confirms that the impact caused damage to the coating surface [1, 24].

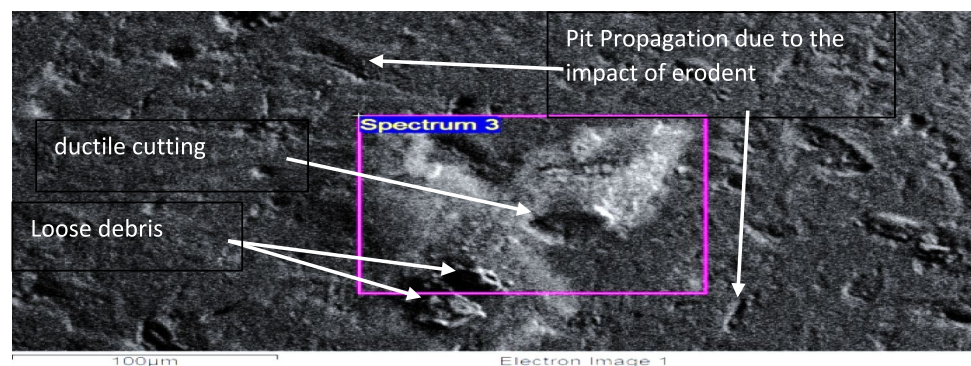
The combination of pit propagation, loose debris, and ductile cutting observed in Fig. 6 provides evidence of the extent of damage caused by the impact under these conditions. The deformation and cutting action caused significant damage to the coating, resulting in the formation of pits and the removal of material, which formed loose debris.

The observation of ductile cutting in Fig. 6 is consistent with the observation in Fig. 5, which suggests that the coating is a ductile material. This information is important for understanding the behaviour of the coating under high-speed impact conditions and for determining the potential applications of the coating in environments with high-velocity impacts [25].

3.4 Erosion Mapping of Surface Coating

To visualise damage, erosion maps were created as an alternative method. The aim of the study was to produce erosion maps and patterns in coated samples using a developed code written in MATLAB. This map allowed for the analysis

Fig. 6 Coated sample at 75 Impact angle and 10.16-m/s velocity



and assessment of the coating erosion process, giving valuable insights into material behaviour under different conditions. Utilising the maps can aid in comprehending erosion mechanisms in coating and composite materials, which can assist design engineers in forecasting safety levels during operation and lead to the creation of a more sturdy and long-lasting coating for tidal turbine blades [26, 27].

The erosion map provides a graphical representation of the level of material loss experienced by the coating under different impact velocities and angles [28]. The map in Fig. 7 indicates that the coating is most resistant to erosion when tested at impact angles of 15°, 30°, 45°, and 75° and velocities of 6.25 m/s, 8.42 m/s, and 10.16 m/s, suggesting that the coating's design is most effective at deflecting the force of the impacting particles when it is applied at these angles.

In contrast, the coating experiences higher levels of erosion when tested at impact angles of 60° and 90° and velocities of 6.25 m/s, 8.42 m/s, and 10.16 m/s, indicating that the design may not be as effective at deflecting the force of particles at these angles. This suggests that design modifications may be necessary to enhance the coating's performance under these impact conditions [29].

Figure 7 revealed that the coating performed best at a velocity of 6.25 m/s compared to velocities of 8.42 m/s and 10.16 m/s. This data can be used to optimise the design of the tidal turbine blades to reduce the impact of ocean currents and tides, potentially reducing erosion and improving the durability of the coating.

The erosion map effectively illustrates the coating's response to various impact conditions, offering a detailed understanding of its performance under specific environmental stresses [30]. By analysing the map, design engineers can determine the optimal impact angles and velocities for the coating, enabling them to optimise the design of the tidal turbine blades for increased durability and longevity [31]. The map's findings can be used to enhance the efficiency and sustainability of harnessing the power of ocean currents and tides through tidal turbines [18].

The study focused on slurry erosion behaviour in coating under simulated tidal turbine conditions but did not

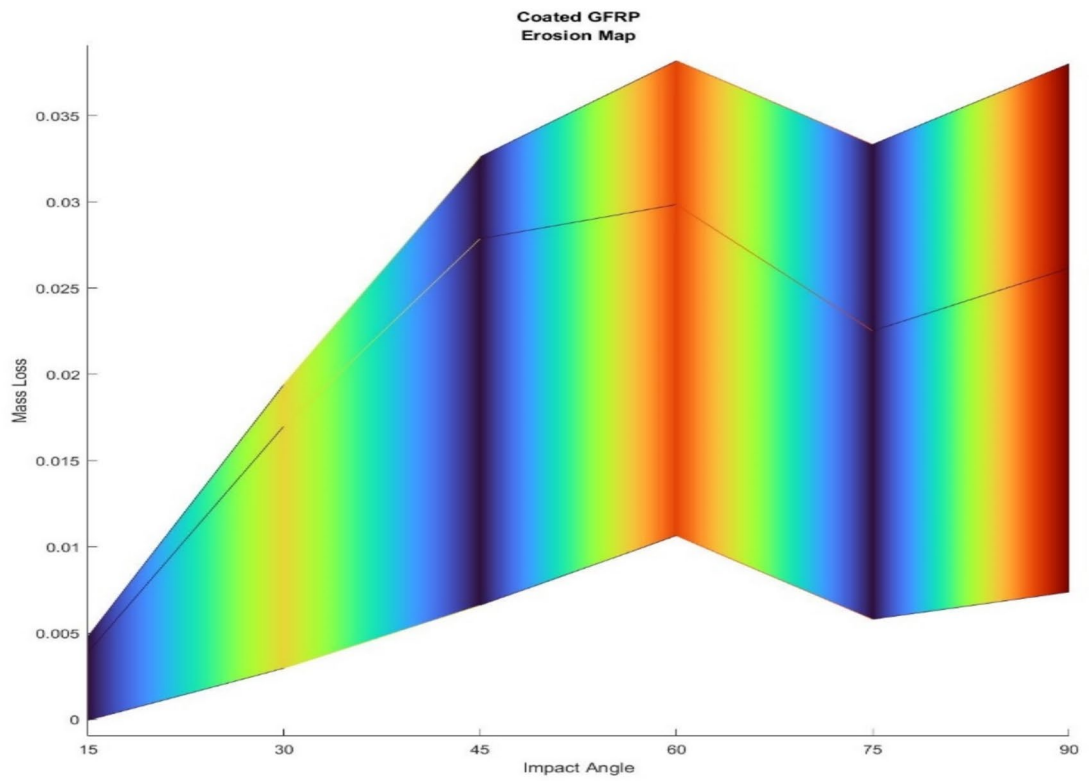
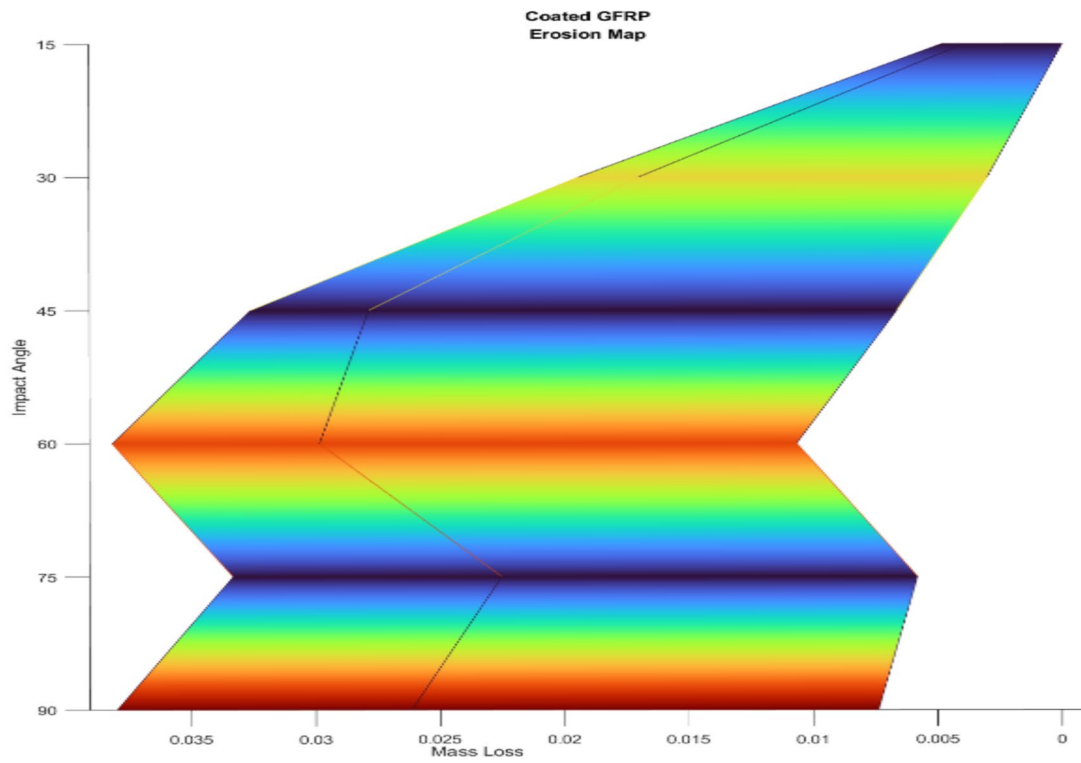


Fig. 7 Erosion map of surface coating

account for cavitation effects. Cavitation, caused by the formation and collapse of vapour bubbles under rapid pressure changes, is a significant degradation mechanism in marine environments. It induces localised stresses and surface fatigue, which can exacerbate material damage. Future studies should incorporate cavitation, either independently or in combination with slurry erosion, to provide a more comprehensive evaluation of material performance.

The study did not assess the long-term erosion performance of the coating under extended exposure to saline conditions and prolonged particle impact. Such factors can affect the coating's erosion resistance, leading to increased material loss and surface degradation. Future research should evaluate these effects to better understand the coating's durability in marine environments.

4 Conclusion

- The study aimed to address the erosion challenges of the coating material used in tidal turbine blades. The study also emphasised the importance of using erosion maps to visualise and analyse the level of material loss under different impact conditions.
- The erosion map produced in the study provides valuable insights into the behaviour of the coating and can be used to optimise the design of tidal turbine blades for increased durability and longevity [3].
- The highest erosion was observed at 75° and 90° impact angles at all impact velocities. The erosion maps displayed the level of material loss experienced by the coating under different impact conditions, offering useful information for the design of tidal turbine blades.

Acknowledgements Emadelddin Hassan generated this paper as part of his PhD work under the supervision of Professor Margaret Stack. He developed the experimental, developed the maps, and generated the textual narrative.

Author Contributions E.H. conducted the experiments and data analysis. M.M.S. supervised the research and contributed to the study design. E.H. and M.M.S. jointly wrote the manuscript. Both authors reviewed and approved the final version of the manuscript.

Funding The authors would like to acknowledge the support of the Interreg (Northern Ireland—Ireland—Scotland) Special EU Programmes Grant No SPIRE2_INT-VA-049 “Storage Platform for the Integration of Renewable Energy (SPIRE 2)”.

Data Availability No datasets were generated or analysed during the current study.

Declarations

Competing interests The authors declare no competing interests.

Ethical Approval Not applicable.

Open Access This article is licensed under a Creative Commons Attribution 4.0 International License, which permits use, sharing, adaptation, distribution and reproduction in any medium or format, as long as you give appropriate credit to the original author(s) and the source, provide a link to the Creative Commons licence, and indicate if changes were made. The images or other third party material in this article are included in the article's Creative Commons licence, unless indicated otherwise in a credit line to the material. If material is not included in the article's Creative Commons licence and your intended use is not permitted by statutory regulation or exceeds the permitted use, you will need to obtain permission directly from the copyright holder. To view a copy of this licence, visit <http://creativecommons.org/licenses/by/4.0/>.

References

1. Rasool G, Stack MM (2019) Some views on the mapping of erosion of coated composites in tidal turbine simulated conditions. *Tribol Trans* 62(3):512–523. <https://doi.org/10.1080/10402004.2019.1581313>
2. Cai LX, Li Y, Sen Wang S, He Y, Li F, Liu ZK (2021) Investigation of the erosion damage mechanism and erosion prediction of boronized coatings at elevated temperatures. *Materials* 14(1):1–18. <https://doi.org/10.3390/ma14010123>
3. Johnstone C, Stack M, Sharifi S, Johnstone C, Stack MM. Tribological challenges of scaling up tidal turbine blades. [Online]. <https://www.researchgate.net/publication/299369786>
4. Ahamed RAR, Johnstone CM, Stack MM (2016) Impact angle effects on erosion maps of GFRP: applications to tidal turbines. *J Bio Tribocorros*. <https://doi.org/10.1007/s40735-016-0044-1>
5. Belzona. <https://www.belzona.com/en/products/2000/2141.aspx>
6. Zu JB, Hutchings IM, Burstein GT (1990) Design of a slurry erosion test rig. *Wear* 140(2):331–344. [https://doi.org/10.1016/0043-1648\(90\)90093-P](https://doi.org/10.1016/0043-1648(90)90093-P)
7. Roshanmanesh S, Hayati F, Papaelias M (2020) Tidal turbines. Non-destructive testing and condition monitoring techniques for renewable energy industrial assets, pp. 143–158. <https://doi.org/10.1016/B978-0-08-101094-5.00010-1>
8. Muratoglu A, Yuce MI (2015) Performance analysis of hydrokinetic turbine blade sections
9. Manwell JF, McGowan JG, Rogers AL (2010) Wind energy explained: theory, design and application
10. National Renewable Energy Laboratory (lead) and Verdant Power. Tidal Power Turbine Demonstrates Thermoplastic Blades. <https://www.energy.gov/eere/water/articles/tidal-power-turbine-demonstrates-thermoplastic-blades>
11. Rasool G, Johnstone C, Stack MM. Tribology of Tidal Turbine Blades: Impact angle effects on erosion of polymeric coatings in sea water conditions
12. Dashtkar A et al (2019) Rain erosion-resistant coatings for wind turbine blades: a review. *Polym Polym Compos* 27(8):443–475. <https://doi.org/10.1177/0967391119848232>
13. Wang S, Liu G, Mao J, He Q, Feng Z (2009) Effects of coating thickness, test temperature, and coating hardness on the erosion resistance of steam turbine blades. *J Eng Gas Turbine Power*. <https://doi.org/10.1115/1.3155796>
14. Hassani S, Klemberg-Sapieha JE, Bielawski M, Beres W, Martinu L, Balazinski M (2008) Design of hard coating architecture for the optimization of erosion resistance. *Wear* 265(5–6):879–887. <https://doi.org/10.1016/J.WEAR.2008.01.021>
15. Stack MM, Jana BD, Abdelrahman SM (2011) Models and mechanisms of erosion–corrosion in metals. *Tribocorrosion of Passive*

- Metals and Coatings, pp. 153–187e. <https://doi.org/10.1533/9780857093738.1.153>
16. Chouhan JS et al (2023) Preliminary investigation of slurry erosion behaviour of tantalum. *Wear* 516–517:204605. <https://doi.org/10.1016/J.WEAR.2022.204605>
 17. Schmitt R (2014) Scanning Electron Microscope. In: Laperrière L, Reinhart G (ed), *CIRP Encyclopedia of Production Engineering*. Springer Berlin Heidelberg, Berlin, Heidelberg, pp. 1085–1089. https://doi.org/10.1007/978-3-642-20617-7_6595
 18. Rasool G, Sharifi S, Johnstone C, Stack MM (2016) Mapping synergy of erosion mechanisms of tidal turbine composite materials in sea water conditions. *J Bio Tribocorros*. <https://doi.org/10.1007/s40735-016-0040-5>
 19. Davies P, Rajapakse YDS, Verdu J (2014) *Durability of composites in a marine environment*, vol 208. Springer, New York
 20. Miller D, Mandell J, Samborsky D, Hernandez-Sanchez B, Griffith DT (2012) Performance of composite materials subjected to salt water environments. In: 53rd AIAA/ASME/ASCE/AHS/ASC Structures, Structural Dynamics and Materials Conference 20th AIAA/ASME/AHS Adaptive Structures Conference 14th AIAA, p. 1575
 21. Ring TA, Feeney P, Boldridge D, Kasthurirangan J, Li S, Dirksen JA, *Brittle and Ductile Fracture Mechanics Analysis of Surface Damage Caused During CMP*
 22. Prashar G, Vasudev H, Thakur L (2020) Performance of different coating materials against slurry erosion failure in hydrodynamic turbines: a review. *Eng Fail Anal* 115:104622. <https://doi.org/10.1016/J.ENGFAILANAL.2020.104622>
 23. Naveed M, Schlag H, König F, Weiß S (2016) Influence of the erodent shape on the erosion behavior of ductile and brittle materials. *Tribol Lett* 65(1):18. <https://doi.org/10.1007/s11249-016-0800-x>
 24. Desale GR, Gandhi BK, Jain SC (2006) Effect of erodent properties on erosion wear of ductile type materials. *Wear* 261(7–8):914–921. <https://doi.org/10.1016/J.WEAR.2006.01.035>
 25. Musavi SH, Davoodi B, Nankali M (2021) Assessment of tool wear and surface integrity in ductile cutting using a developed tool. *Arab J Sci Eng* 46(8):7773–7787. <https://doi.org/10.1007/s13369-021-05560-4>
 26. Sloan J, Stack M (2020) On the construction of raindrop erosion maps for steel
 27. Hassan E et al (2021) Erosion mapping of through-thickness toughened powder epoxy gradient glass-fiber-reinforced polymer (GFRP) plates for tidal turbine blades. *Lubricants*. <https://doi.org/10.3390/lubricants9030022>
 28. Stack MM, Corlett N, Zhou S (1996) Construction of erosion-corrosion maps for erosion in aqueous slurries. *Mater Sci Technol* 12:662–672
 29. Patel M, Patel D, Sekar S, Tailor PB, Ramana PV (2016) Study of solid particle erosion behaviour of SS 304 at room temperature. *Procedia Technol* 23:288–295. <https://doi.org/10.1016/j.protcy.2016.03.029>
 30. Rasool G, Middleton AC, Stack MM (2020) Mapping raindrop erosion of GFRP composite wind turbine blade materials: perspectives on degradation effects in offshore and acid rain environmental conditions. *J Tribol*. <https://doi.org/10.1115/1.4046014>
 31. Algaddaime TF, Hassan E, Stack MM (2024) Investigating the Performance of Glass Fibre-Reinforced Polymer (GFRP) in the Marine Environment for Tidal Energy: Velocity, Particle Size, Impact Angle and Exposure Time Effects

Publisher's Note Springer Nature remains neutral with regard to jurisdictional claims in published maps and institutional affiliations.